Journal of Analytical and Applied Pyrolysis 181 (2024) 106569

Contents lists available at ScienceDirect

Journal of Analytical and Applied Pyrolysis

journal homepage: www.elsevier.com/locate/jaap

Exploring molecular composition of upgraded pyrolysis bio-oil using GC×GC-(EI/PI)-TOF MS with different column set-ups

Eliane Lazzari [a,b,c], Charlotte Mase [a,b], David C. Dayton [d], Sabrina Marceau [a,b], Giorgia Purcaro [e], Jean-François Focant [c], Marco Piparo [a,b,*], Pierre Giusti [a,b]

[a] TotalEnergies One Tech, R&D, Downstream Processes & Polymers, TotalEnergies Research & Technology Gonfreville, BP 27, Harfleur 76700, France
[b] International Joint Laboratory, iC2MC: Complex Matrices Molecular Characterization, TRTG, Harfleur, France
[c] Organic and Biological Analytical Chemistry Group, MolSys Research Unit, University of Liège, Liège, Belgium
[d] RTI International, Technology Advancement and Commercialization, 3040 E. Cornwallis Road, Research Triangle Park, NC 27709, USA
[e] Gembloux Agro-Bio Tech, University of Liège, Gembloux, Belgium

ARTICLE INFO

Keywords:
Gas chromatography
Pyrolysis
Bio-oils
GC×GC

ABSTRACT

Bio-oils produced from the pyrolysis of lignocellulosic biomass are rich in oxygen, which causes instability and corrosion problems. Therefore, dedicated post-pyrolysis treatments such as hydrotreatment are required to increase the H/C ratio of the products to be used as fuel or chemicals. Here, a characterization method based on two-dimensional gas chromatography (GC×GC) was developed to highlight the evolution of the volatile fraction during hydrotreatment. Six samples obtained at different times of the hydrotreatment were analyzed. In this way, information on catalyst deactivation was obtained. The combination of information from normal and reversed phase GC×GC analysis provides a detailed characterization of the hydrotreated bio-oils. Furthermore, the use of soft photoionization (PI), in addition to conventional electron impact ionization (EI), yields a better understanding of the compound structures present in the sample. Identification and semi-quantification of the sample components indicate that the concentration of paraffins, cycloalkanes, and monoaromatics have largely decreased during hydrotreatment, while the concentration of oxygenated species and polycyclic aromatic hydrocarbons have increased. Using complementary GC methods highlights changes in the molecular composition of volatile species that correlate with catalyst performance. This approach can be used to follow the decrease in hydrodeoxygenation activity as a function of time on stream to estimate the catalyst aging during the hydrotreating process.

1. Introduction

As the energy transition continues, the search for new energy resources for producing transportation fuels with similar performance to petroleum-based fuel remains a primary challenge. The widespread availability of biomass logically makes it a good candidate for meeting alternative transportation fuel demands with lower greenhouse gas emissions to reduce global warming. Thermochemical conversion processes, including pyrolysis, can be used to convert biomass into biofuels [1].There are several types of pyrolysis processes that can be differentiated by process conditions and the use of catalysts, such as fast pyrolysis [2] and catalytic fast pyrolysis [3]. Both are characterized by high heat transfer rates and short residence time. However, bio-oils produced from conventional thermal and catalytic biomass pyrolysis contain a high concentration of oxygenated components that are reactive and thermally unstable, negatively impacting the physiochemical properties of the produced bio-oils. The chemical composition of such bio-oils can be significantly modified by adding a reactive gas, such as hydrogen, during the catalytic pyrolysis process to promote selective hydrodeoxygenation (HDO) and reduce char formation [4–6]. The reactive catalytic biomass pyrolysis process yields bio-oils that generally contain less oxygen and significantly more hydrocarbons than the thermal or catalytic bio-oils [7] using the same biomass feedstock, however, oxygen-containing molecules are not completely eliminated. Therefore, to produce biofuels, similar to petroleum-based fuels, from bio-oils requires an additional upgrading step to remove residual

* Corresponding author at: TotalEnergies One Tech, R&D, Downstream Processes & Polymers, TotalEnergies Research & Technology Gonfreville, BP 27, Harfleur 76700, France.
E-mail address: marco.piparo@totalenergies.com (M. Piparo).

https://doi.org/10.1016/j.jaap.2024.106569
Received 14 February 2024; Received in revised form 18 April 2024; Accepted 29 May 2024
Available online 3 June 2024

refractory oxygen compounds. HDO is commonly used to reduce the oxygen content of bio-oils, resulting in lower acidity and improved thermal stability [8,9]. In this process, oxygenated molecules are converted to aliphatic and aromatic compounds using high-pressure hydrogen in the presence of a catalyst.

Developing efficient upgrading processes requires a comprehensive understanding of the chemical composition of the complex bio-oil intermediates, which can only be achieved using advanced analytical techniques. The many techniques reported in the literature for characterizing bio-oils [10,11] can be divided into two classes according to the information that they generate: (i) molecular and structural information can be obtained using mass spectrometry (MS), liquid chromatography (LC), and gas chromatography (GC) methods while (ii) functional skeletal information can be obtained using Fourier transform infrared spectroscopy (FTIR) and nuclear magnetic resonance (NMR) methods. At the molecular level, direct infusion high-resolution MS (HRMS) is widely used to characterize the non-volatile and high molecular weight compounds in bio-oils [12]. The characterization of volatile compounds is carried out by coupling (HR)MS to GC, which is currently the most widely used technique, providing qualitative and quantitative information.

Conventional one-dimensional (1D) GC can be used to characterize volatile compounds in bio-oil [11,13–16]. However, this method has limitations due to the limited peak capacity. Several co-elution phenomena can occur, resulting in inaccurate quantification and less accurate and less comprehensive sample characterization. Advanced GC techniques, such as two-dimensional GC (GC×GC), is one of the most efficient techniques to analyze complex organic mixtures and it has become one of the most promising analytical approaches for comprehensive bio-oil analysis [17]. The combination of two different columns provides an additional dimension of chromatographic separation [17,18] compared to conventional 1D GC. Higher peak capacity, enhanced sensitivity, and well-structured 2D chromatograms are obtained enabling a more in-depth molecular characterization. A comprehensive discussion of the use of GC×GC in the field is out of the scope of this paper, but readers are directed toward two recent reviews [18,19].

According to the nature of the combined GC stationary phases, GC×GC column sets can be configured in the normal or reversed phase [18]. Typically, the normal phase configurations consist of a non-polar or weakly polar column in the first dimension and a much shorter polar column in the second dimension. This configuration effectively separates saturated and aromatic compound classes. Conversely, reversed-phase configurations consist of a polar column installed in the first dimension and a non-polar column in the second dimension for better separation of saturated compounds and polar oxygenated compounds [18,20–22].

Omais *et al.* tested four-column combinations in both normal and reversed phases to characterize hydrotreated bio-oils [23]. They showed that the best separation of oxygenated and hydrocarbon compounds was achieved using 100 % polyethylene glycol and phenyl/PSPS (50/50) in the first and second dimensions, respectively. However, this column combination leads to some bleeding at higher temperatures. In another study, Djokic *et al.* reported significant co-elution of aldehydes, ketones, and furans when characterizing thermal bio-oil and its hydrotreated effluents using the normal phase configuration, which was subsequently improved using the reversed-phase configuration [20].

The combination of both electron impact ionization (EI) and photoionization (PI) sources with both normal and reversed phase 2D GC provides complimentary measurements, leading to more detailed characterization with improved species identification. Accurate structural information for the analysis of complex hydrocarbon mixtures using PI has been reported in the literature [24,25]. Lazzari *et al.* recently reported the great potential of using GC×GC-PI-time-of-flight (TOF) MS and GC-vacuum ultraviolet (VUV) detection for the chemical analysis of recycled plastic pyrolysis oils [26].

The aim of this study is to evaluate the HDO process for upgrading reactive catalytic fast pyrolysis bio-oil by utilizing qualitative and semi-quantitative approaches to characterize six hydrotreated effluents collected at different time points. The first part will focus on the optimization method using one effluent to highlight the important contribution of comprehensive GC×GC for the characterization of volatile molecules. In the second part, the detailed chemical characterization of the six HDO effluents from the same HDO process collected at different treatment times using the GC×GC method will be compared to highlight the evolution of the chemical compositions as the HDO catalytic activity decreased.

2. Materials and methods

2.1. Bio-oil production and upgrading

Samples were supplied by RTI International, North Carolina, United States. Bio-crude oil was obtained from the reactive catalytic fast pyrolysis (RCFP) of loblolly pine [4,5]. The process was performed under 80 vol% hydrogen in a laboratory-scale pyrolysis reactor (2.5 in diameter fluidized bed reactor) with molybdenum-based catalyst, at an average temperature of 500 °C and biomass feed rate of about 4–5 g per minute. The RCFP bio-crude obtained was subsequently hydrotreated continuously for 144 hours in RTI's pilot-scale hydroprocessing unit at 2000 psi of hydrogen pressure and a liquid hourly space velocity (LHSV) of 0.35/hr over a sulfided hydrotreating catalyst. The average reactor bed temperature was 300 °C, with 9.0 kg of RCFP bio-crude feed processed. Six samples were recovered at different time points: ~36.5, 48.5, 72.5, 96.5, 124.5, and 143.5 hours and were namely HDT-RCFP #1 to #6 respectively [5].

The HDT-RCFP-1 recovered at 36.5 hours was used for analytical condition optimization and to create a characterization template to apply to the other samples. All HDT-RCFP samples were injected without previous dilutions. RCFP bio-crude has not been analyzed by GC due to the presence of a significant amount of high boiling point compounds identified in an earlier analytical screening [27].

2.2. GC×GC analysis

The HDT-RCFP samples were analyzed using two independent GC×GC-MS systems equipped with different ionization modes (EI and PI). Details on the instrumentation and conditions are described below.

2.2.1. GC×GC-EI-QTOF MS Instrumentation

The GC×GC-EI-QTOF MS instrument combined an Agilent 7890 A gas chromatography with a PTV injector (Agilent Technologies, Inc, CA, USA) and a ZOEX ZX2 cryogenic modulator (Houston, TX, U.S.A.) interfaced with an EI ion source coupled to the QTOF mass spectrometry detector (7250 Agilent). With this system, two column sets were investigated: a normal phase (non-polar × mid-polar) and a reverse phase (mid-polar × non-polar). The detailed information on column characteristics and GC×GC analytical conditions used for both column sets are listed in Table 1.

The modulation loop was made using a deactivated silica column (1 m × 0.25 mm i.d.). In the QTOF MS the interface and ion source temperatures were set at 250 and 225 °C, respectively. A mass range of *m/z* 45–450 was collected with an acquisition rate of 50 spectra/s.

2.2.2. GC×GC-PI-TOF MS Instrumentation

The soft ionization GC×GC measurements were conducted using an Agilent 7890B GC equipped with an OPTIC-4 injector (GL-Sciences BV, Eindhoven, The Netherlands) and a ZX2 cryogenic modulator (Zoex Corp. Houston, TX, U.S.A.). interfaced with a PI/EI combination ion source coupled to the TOF MS detector (JMS-T200GC "AccuTOF GCx-plus", JEOL Ltd., Tokyo, Japan. A deuterium lamp was the source of 118 nm photons to achieve soft (10.78 eV) single-photoionization. Further technical details on the PI are described elsewhere [28]. A

Table 1
Chromatography conditions used for normal and reversed GC×GC-EI-QTOF MS analysis.

Feature	Normal GC×GC-EI-QTOF MS	Reversed GC×GC-EI-QTOF MS
1st column	TG-5HT- Thermo Fisher Scientific (60 m × 0.25 mm i.d. × 0.25 μm d_f)	ZB-35HT inferno – Phenomenex (30 m × 0.25 mm i.d. × 0.25 μm d_f)
2nd column	DB-17HT (Agilent J & W technology) (2 m × 0.25 mm i.d. × 0.25 μm d_f)	RXI-1 ms - Restek Corporation (2 m × 0.1 mm i.d. × 0.1 μm d_f)
Oven program	70 °C (1.5 °C min^{-1}) to 320 °C	70°C - 5 min (1.5 °C min^{-1}) to 320 °C
PTV inlet program	120 °C (100 °C.min^{-1}) to 200 °C (200 °C.min^{-1}) to 350 °C	
Injection size and split ratio	0.5 μL (1:300)	0.5 μL (1:300)
Carrier gas flow	He (1 mL min^{-1})	He (1.5 mL min^{-1})
Modulation period	12 s (hot jet 0.6 s)	6.5 s (hot jet 0.6 s)

normal phase (non-polar × mid-polar) column set was used. The ^{1}D column was Rxi-5MS (30 m × 0.25 mm i.d. × 0.25 μm Restek Corporation) and the ^{2}D column was Rxi-17Sil MS (1.5 m × 0.25 mm i.d. × 0.25 μm df, Restek Corporation). The modulation loop was made using a deactivated silica column (1 m × 0.25 mm i.d.) and the modulation period was 12 s with a hot jet of 0.4 s. Other optimized conditions were as follows. The hot injection temperature was 280 °C, with an injection of 1 μL in a split mode (split ratio 1:80). Helium was used as carrier gas at a flow rate of 1 mL min^{-1}. The GC oven temperature was set at 40 °C (0.2 s), then increased to 280 °C (hold 2 min) at 3 °C min^{-1}. Interface and ion source temperatures were set at 200 °C and 300 °C, respectively. A mass range of *m/z* 45–450 was collected with an acquisition rate of 50 spectra/s.

2.2.3. Qualitative and semi-quantitative analysis

Data produced were processed using GC Image® v 2.3 (Zoex Corp.) and ChromSpace® (SepSolve, Peterborough, U.K), including tools to generate extracted ion current chromatograms (EIC). EIC filters were used to facilitate the vizualization of different chemical classes in the 2D chromatogram. The tentative identification of compounds was achieved by combining the EI and PI spectrum data. Spectrum from EI, at 70 eV, were compared to the NIST library database, and a minimum of 70 % spectral match quality was considered for compound identification. On the contrary, PI spectra were used to confirm the molecular ion and the tentative identifications performed with the EI system. A semi-quantitative approach (percent area %) was described for each chemical class by summing the area of the peaks belonging to a specific chemical class and comparing it to the total area of the sample peaks.

3. Results and discussion

Due to the complexity of the sample, exploiting complementary GC column combinations and structural information determined using soft and hard ionization methods can make comprehensive sample characterization less challenging. Conventional normal (non-polar × mid-polar) and reversed (mid-polar × non-polar) column sets were both used to perform GC×GC separations, and TOF MS with soft (PI) and hard (EI) ionization were implemented to identify the volatile compounds in the HDT-RCFP samples and create an identification template to apply to the remaining samples.

3.1. Exploring molecular composition of HDT-RCFP #1

Analytical methods were optimized using HDT-RCFP #1 as the benchmark sample.

3.1.1. GC×GC-TOF MS using a conventional normal phase set-up

Initially, a normal phase column set with high thermal stability (TG-5HT *vs* DB-17HT) was selected due to the high boiling points of many components in the HDT-RCFP samples.

3.1.1.1. Use of EI ionization source. Fig. 1a shows the separation by GC×GC-EI-TOF MS using a conventional normal phase set-up for the HDT-RCFP #1. The 2D plot obtained with this configuration shows the complexity of the sample. The EIC shown in Fig. 1b, 1c, 1d, and 1e were used to assign the chemical classes to the analytes present. Specific fragments for each chemical class were chosen according to the information currently available in the scientific literature. For example, Shimoyama and Yabuta [29,30] and Alam *et al.* [31] have used *m/z* 69, 83, 97, and 111 for the identification of the one-ring cycloalkanes family, and *m/z* 67, 81, and 95 for the identification of the two-ring cycloalkanes. For the aromatics and diaromatics families, *m/z* 91 and *m/z* 128 were used for their identification. Finally, *m/z* 107, 122, 136, 150, and 164 were selected for the phenol group type.

Fig. 1b shows the EIC for the cycloalkanes family. Regarding the elution pattern of the different chemical groups, the cycloalkanes elute in two distinct elution bands. The first one shows the elution of the one-ring cycloalkanes, and the second one the two-ring cycloalkanes. Both are ordered by the degree of branching and the length of the alkyl group attached to the ring.

The EIC shown in Fig. 1c is for monoaromatics identified by monitoring the tropylium ion (*m/z* 91), a well-known fragment for molecules with one carbon atom attached to a benzene ring. The elution pattern of the monoaromatics is a function of the number of carbons, the degree of branching, and the presence of unsaturation of the alkyl group attached to the benzene nucleus.

Different PAH compounds found in HDT-RCFP #1 were identified by characteristic molecular ions at *m/z* 128, 166, and 178 for naphthalene, fluorene, and phenanthrene/anthracene, respectively. Diaromatic compounds, including alkylated derivatives of naphthalene, are highlighted in Fig. 1d. The EIC of the fluorene, its derivatives, and phenanthrene/anthracene compounds are shown in Figure S1.

Finally, the EIC of the ions *m/z* 107, 122, 136, 150, and 164 facilitated the identification of the chemical class of the phenols, as shown in Fig. 1e. A clear cluster based on the number of carbons of the alkyl group attached to the phenol nucleus (*i.e.*, C1 to C7 phenol isomers) was identified. This group of compounds coeluted with the diaromatic class but can be easily identified using the specific fragment ions.

3.1.1.2. Insights on PI spectra for bio-oil qualitative screening using conventional normal phase set-up. In this work, PI was used to confirm the identification of chemical classes. Indeed, PI is considered a soft ionization technique that reduces fragmentation and preserves the parent molecular ion compared to EI, where greater fragmentation and the loss of molecular ions result in more complicated and potentially ambiguous species identification. Fig. 2 compares mass spectra using EI *vs.* PI for several groups of compounds. Please note that even if the authors decided to use two different column sets and oven program temperatures in the two experiments (PI *vs.* EI), no major differences were observed in the 2D chromatograms. The 2D color plots shown here are an expansion of the EICs shown in Fig. 1. Although the two column set-ups are different, the identification of the compounds is possible thanks to the mass and the well-structured 2D chromatograms. As expected, the molecular ion ($M^{+\bullet}$) was the dominant peak in the PI spectrum, while some chemical classes did have certain fragment patterns that were different from those observed in the EI spectra.

For cycloalkanes (Fig. 2a), the resulting PI mass spectrum showed the presence of characteristic ring fragment ions, *m/z* 96 and 110 [28], and dominant molecular ions. Using the information determined from the PI, congeners of C5-cyclohexanes with alkyl substituents were grouped under a molecular ion at *m/z* 154, while two-ring

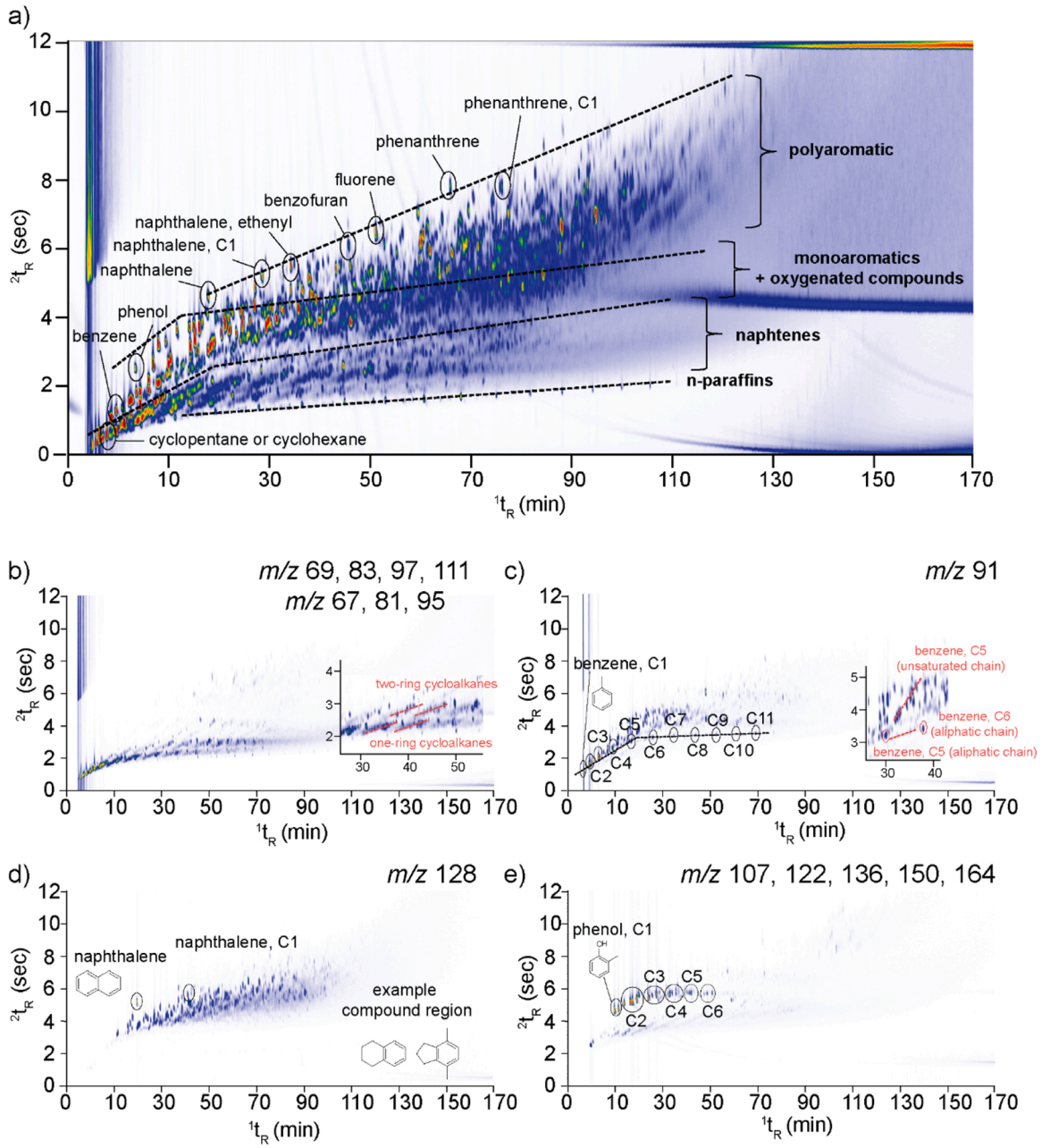

Fig. 1. (a) GC×GC-EI-TOF MS total ion chromatogram (TIC) of the HDT-RCFP #1, showing the separation of the conventional normal (non-polar × polar) column set-up under optimized conditions. Extracted ion chromatograms of HDT-RCFP #1 from GC×GC-EI-TOF MS using conventional normal (non-polar × polar) column set-up, illustrating the detection of (b) cycloalkanes (c) mono-aromatics, (d) di-aromatics and (e) alkyl-phenols.

C5-cyclohexane congeners were assigned to the molecular ion at *m/z* 152. It is also noteworthy that the cycloalkane structures identified are different from those typically found in petroleum-based products. Unlike fused cyclohexane rings that share two carbons, the lignin-based cycloalkanes mainly belong to the bi-cyclohexyl alkane family, where bridge aliphatic alkane connects two cyclohexane rings [32]. The ring fragments that appear in the PI spectra (*m/z* 96 and 110) are also consistent with this cycloalkane type of structure. PI may not be energetic enough to cleave two fused rings, as reported by Giri *et al.* in a base oil analysis [28]. These authors show PI spectra for three different groups of fused bicyclic alkanes, and in none of them were ring fragments detected as in the present study.

The intensity of the monoaromatic parent ions was enhanced using PI (Fig. 2b) making it easier to group the compounds according to the length of the unsaturated carbon chain attached to the benzene ring. The molecular ion at *m/z* 148 confirmed the aliphatic (branched) chain congeners of C5-benzene, and the assignment of the unsaturated (branched) chain congeners of C5-benzene was also confirmed by the molecular ion at *m/z* 146.

The advantage of using PI compared to EI is that PI can produce unique fragment patterns, allowing the assignment of isomer structures in alkyl-series compounds. This is clearly shown in Fig. 2c where the PI mass spectra of C3-alkylphenol isomers are shown. In addition to the molecular ion, two distinct small fragments may guide in deducing the C3-alkylphenol isomer. The fragment at *m/z* 107 suggests a loss of an ethyl group (-C_2H_4) from an ethyl-phenol compound. In the other spectra, a dimethylphenol compound can be rationalized by the loss of the methyl group (-CH_3), fragment with *m/z* 122.

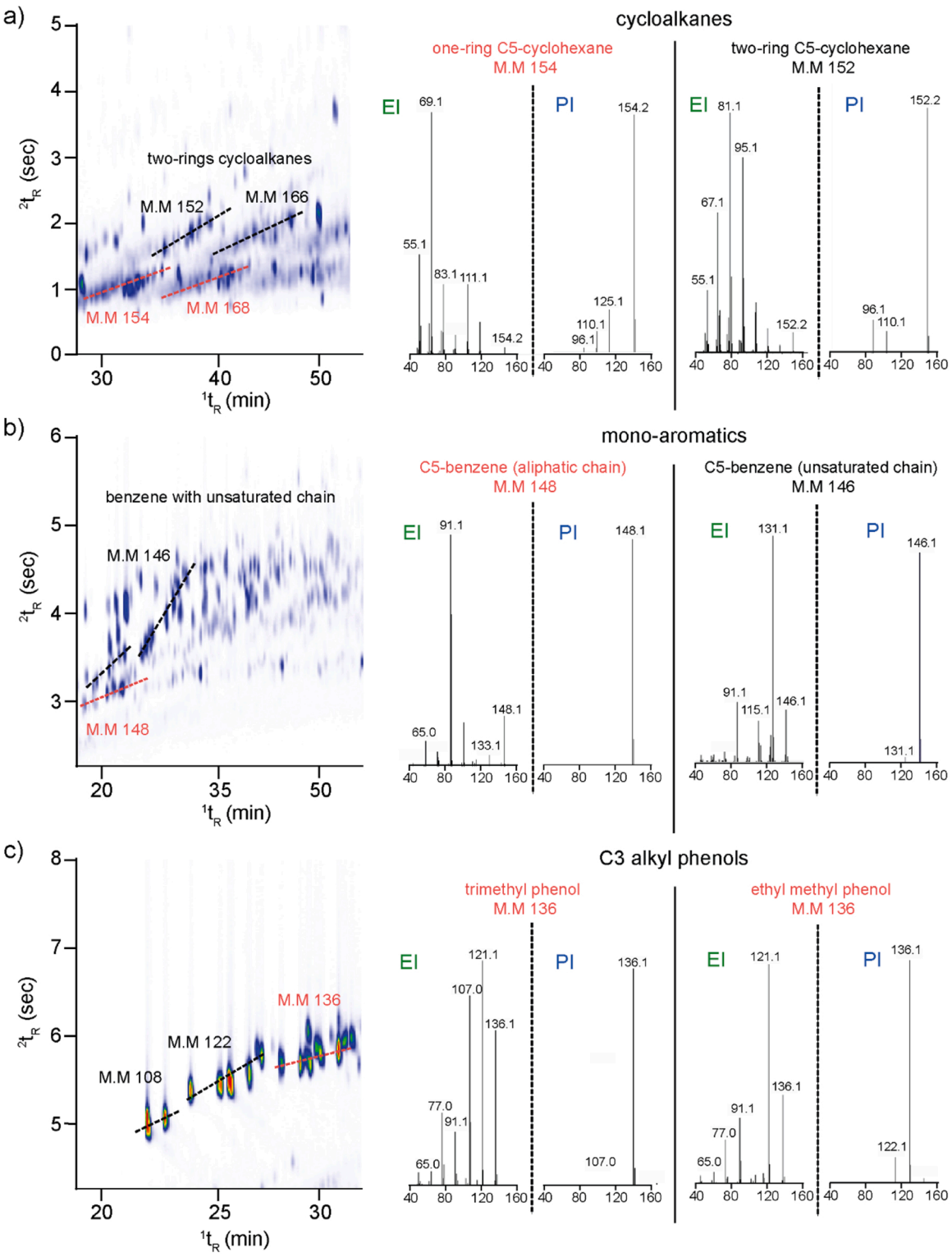

Fig. 2. On the left side, the beginning portion (Fig. 1) of the EIC for HDT-RCFP #1 analyzed by GC×GC-PI-TOF MS using a conventional normal (non-polar × polar) column set-up. On the right side, mass spectra comparing EI vs PI for selected (a) cycloalkanes, (b) mono-aromatics, and (c) alkylphenols.

3.1.2. GC×GC-TOF MS using reverse phase set-up

The goal of bio-oil HDO is to minimize the oxygen content while maintaining a high carbon yield during the upgrading processes. Therefore, the complete characterization of oxygenated compounds in these fluids is of paramount importance. In the normal phase set-up, oxygenated compounds coelute with neighboring peaks (i.e. mono-aromatics such as, for example, monoalkylbenzene or dialkylbenzene), which can mask their identity. The reverse-phase configuration modifies the positional trends so oxygenated compounds elute at lower retention times in the chromatogram, apart from other chemical classes, and facilitate their identification. A configuration using a more polar column in the first dimension and a non-polar column in the second dimension has been shown to separate O-compounds present in a coal-derived hydrocarbon matrix, including the first identification of diols and

naphthalenones [33]. A reversed-phase configuration was also used to improve the group-type analysis of O-compounds in the highly oxygenated bio-oil matrix by Joffres *et al.* [34].

A high thermal stability reversed phase set with a moderately polar column (ZB-35HT) and a second non-polar short column (Rxi-1 ms) was evaluated to improve the characterization of oxygenated compounds in the HDT-RCFP samples. As shown in Fig. 3, the chromatogram is completely different from the chromatogram generated using the normal phase configuration shown in Fig. 1. Here, the *n*-paraffins are eluted in the top elution band of the chromatogram, followed by the elution of the homologs of the cycloalkane isomers in the middle. The separation of the mono- and polyaromatic groups was deteriorated due to the less optimized analytical conditions and the orthogonality set-up. However, the separation of oxygenated compounds was improved. All peaks eluting at the bottom section of the chromatogram with retention times < 70 min were identified as oxygenated compounds. Indeed, these species no longer coelute with nearby families. Zooming in on the carbon region between n-C10 and n-C19 (Fig. 3b), the oxygenated compounds were chromatographically better separated from the hydrocarbon compounds compared to the normal phase set-up.

Chemical classes were assigned using the EIC, in the same way the normal phase configuration data was analyzed. *m/z* 107, 122, 136, 150, and 164 were selected to confirm the identification of alkylphenols (Fig. 3c). Ten peaks were attributed to C3-phenol compared to only four that were identified in the normal phase set-up. Additional alkylphenol isomers were detected along with minor families identified as derivatives of indanone, indenol, naphthalenol, naphthalenone, benzaldehydes, and dibenzofuran (structures highlighted in Fig. 3d). These were not detected with the normal phase set-up. Finally, a nitrogen-containing compound was also identified (number #2).

In the GC×GC experiments using the reversed column set, the improvement in the separation of cycloalkanes is also noteworthy and consistent with the results of Yang *et al.* [32]. This column configuration allowed a better 2D occupation space for this class, providing a higher level of information on the sample composition of the cycloalkane family. Although the chromatogram obtained is well structured, only 48 % of the entire 2D space is used with reverse phase configuration. According to Yang *et al.* [31], this could be due to either 1) partial correlation between the two dimensions or 2) non-optimized 2D column conditions. On the contrary, 76 % of the 2D space was occupied using the normal phase configuration [35,36].

It should be noted that orthogonality itself was not a target. Success is determined by the sufficient separation of the target analytes, which was achieved with the reversed phase approach. For example, better separation of the one-, two-, and three-ring cyclohexanes family (ranging between n-C11 and n-C18) is highlighted compared to the normal phase set-up. *m/z* 67, 69, 81, 83, 95, and 97 were used in EIC for their identification (Fig. 3e). The one-ring, two-ring, and three-ring cyclohexane families are separated in one dimension, while there is a clear order in the second dimension based on the length of the alkyl group attached to the ring.

3.2. Composition of the hydrotreated effluents HDT-RCFP #1 to HDT-RCFP #6 by GC×GC-EI-TOF MS

The results shown above for HDT-RCFP #1 demonstrate that for this type of sample, the 2D reversed phase approach is the most appropriate for identifying the volatile compounds related to catalyst efficiency and deactivation. The approach and methods used for characterizing HDT-RCFP #1 were applied to analyzing the other five samples obtained during the continuous hydroprocessing of the bio-crude produced from loblolly pine. Six hydrotreated products were collected at different times during the 144-hour campaign. A detailed characterization of the non-volatile compounds in these samples was reported by Chacon *et al.* [27]. The reverse phase set-up described in this study was used to characterize the same six samples with a focus on the oxygenated compounds to investigate the change in chemical composition as the hydrodeoxygenation activity of the hydrotreating catalyst decreases.

Fig. 4b shows the GC×GC color maps for HDT RCFP #6, effluents collected at 144 hours of the hydrotreatment process, respectively. Compared to the first effluent, 144 hours of hydrotreatment (HDT-RCFP #6) produced a bio-oil with increased content of volatile oxygenated compounds. Indeed, a higher concentration of oxygenated compounds was observed at the bottom part of the chromatogram in the HDT-RCFP #6. Primarily, a higher number of isomers were found for indanone, indenol, naphthalenol, naphthalenone, and dibenzofuran compounds. In addition, biphenyl compounds that were not present in the first effluent were identified throughout the chromatogram.

The EIC of the alkylphenols family for HDT-RCFP #6 is shown in Fig. 4b. *m/z* 107, 122, 136, 150, and 164 were selected for their identification. This figure can directly be compared to the EIC of the alkylphenols family in HDT-RCFP #1 shown in Fig. 3c.

A higher concentration of oxygenated compounds in the final effluent suggests that the HDO activity of the catalyst decreased during the hydrotreatment process. However, the hydrocarbon fraction is also crucial in determining the effectiveness of biofuel production. The normal phase configuration is most appropriate for focusing on the hydrocarbon compounds. The normal phase GC×GC results obtained for all six hydrotreated effluents (HDT-RCFP #1 to #6) are shown in Figure S2. The resulting 2D-color plots are all very similar, suggesting that while the HDO activity of the hydrotreating catalyst may decrease, the composition of the hydrocarbon fraction of the upgraded products is not significantly affected.

The compounds present in the samples were assigned to paraffins, cycloalkanes, monoaromatics, polycyclic aromatics hydrocarbons (PAHs), and alkylphenols. The assignment of the chemical classes to the analytes in the samples was achieved by displaying EICs (as reviewed in topic 3.1) and a semi-quantitative approach (percent area) was used for comparing the six effluent samples in terms of chemical class distribution. This semi-quantitative analysis was accessed by summing the area % of the peaks assigned, through the EIC, to the different chemical classes and used to compare the chemical class distribution among the effluents. A semi-quantitative analysis has been referred to instead of quantitative since the analysis using GC-MS is more complex and, consequently the prediction of RRF more difficult; oppositely to GC-FID analysis. One of the main reasons for this difficulty is the large variety of GC-MS instrument types and their greater complexity. Fig. 5 shows the distribution of the chemical classes in terms of percent area for all HDT-effluents, including the number of peaks detected in each sample [37].

A semi-quantitative approach was used to compare the chemical class distribution among the effluents and the results are shown in Fig. 5. HDT effluents show a composition predominantly of hydrocarbons and a small part of oxygen compounds. While the identity of the hydrocarbons is consistent from sample to sample, the relative concentrations of these families vary based on the duration of the hydrotreatment. Among the hydrocarbon classes, cycloalkanes showed a 3-fold decrease at longer times on stream. Similarly, a small decrease in the relative concentration of mono-aromatics was observed - 30 % for HDT-RCFP#1 and 20 % for HDT-RCFP#6. Conversely, the concentration of PAHs increased from 45 % in HDT-RCFP#1–70 % in HDT-RCFP#6. The same trend was observed for oxygen compounds that represented only 4 % in HDT-RCFP#1 and 12 % in HDT-RCFP#6. These results suggest that as the activity of the hydrotreating catalysts decreases as a function of time on stream, the relative concentration of oxygenates and PAHs increase as the relative concentration of paraffins, cycloalkanes, and mono-aromatics decrease. It is worth noting that after 72 hours of catalyst use (HDT-RCFP#3), the relative abundance of cycloalkanes dropped precipitously with a sharp increase in PAHs. This observation agrees with the work of Chacon *et al.* who reported the composition of the HDT-RCFP by FTICR MS and suggested a catalyst deactivation around of 72 hours [27].

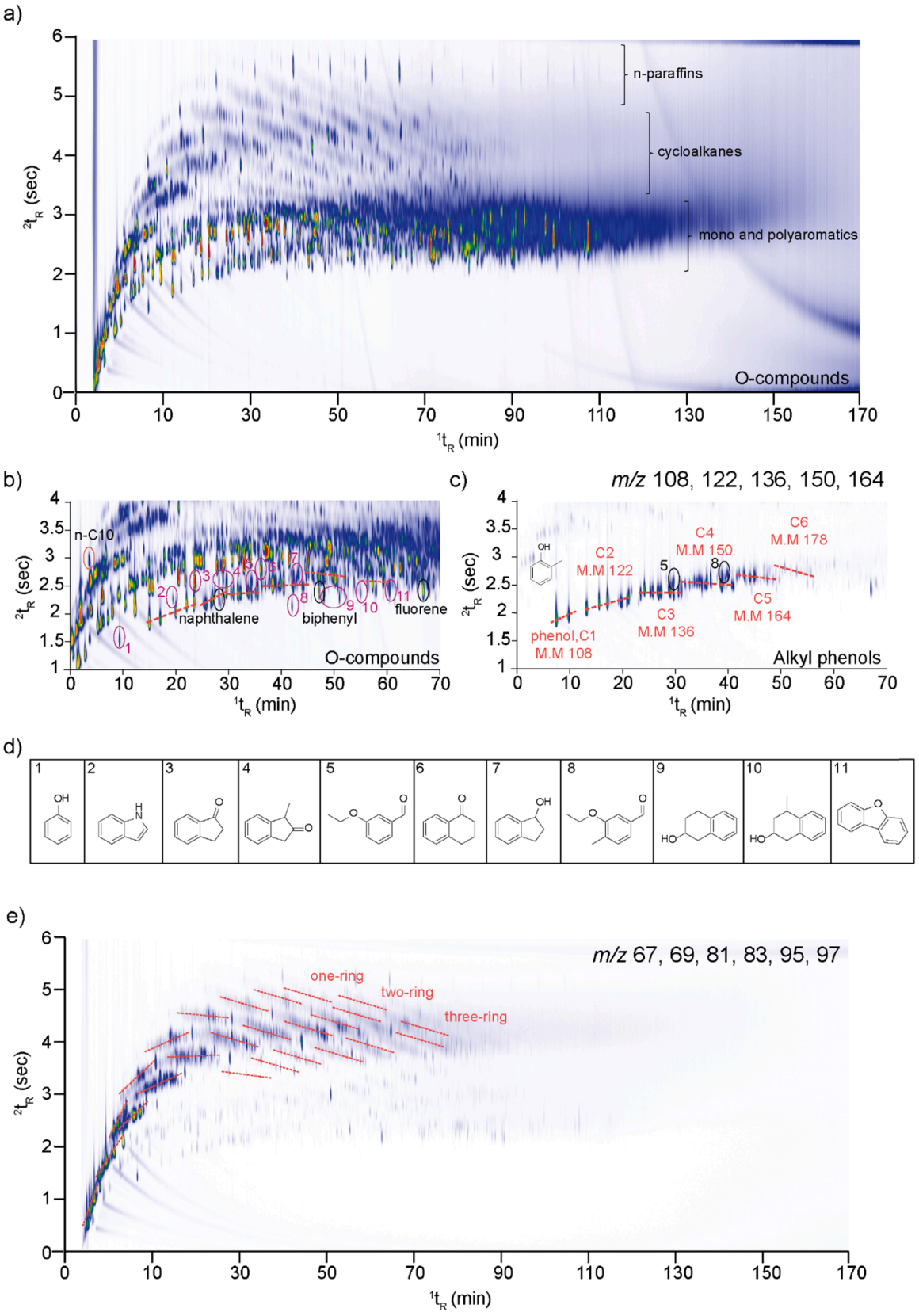

Fig. 3. (a) GC×GC-EI-TOF MS total ion chromatogram (TIC) of the HDT-RCFP #1, using the reverse (mid-polar × non-polar) column set-up under optimized conditions. (b) Isolated carbon region between n-C10 and n-C19. (c) Extracted ion chromatograms (EIC) illustrating the detection of alkyl phenols. (d) Examples of structures of the oxygenated compounds identified. (e) Extracted ion chromatograms showing the detection of cycloalkanes.

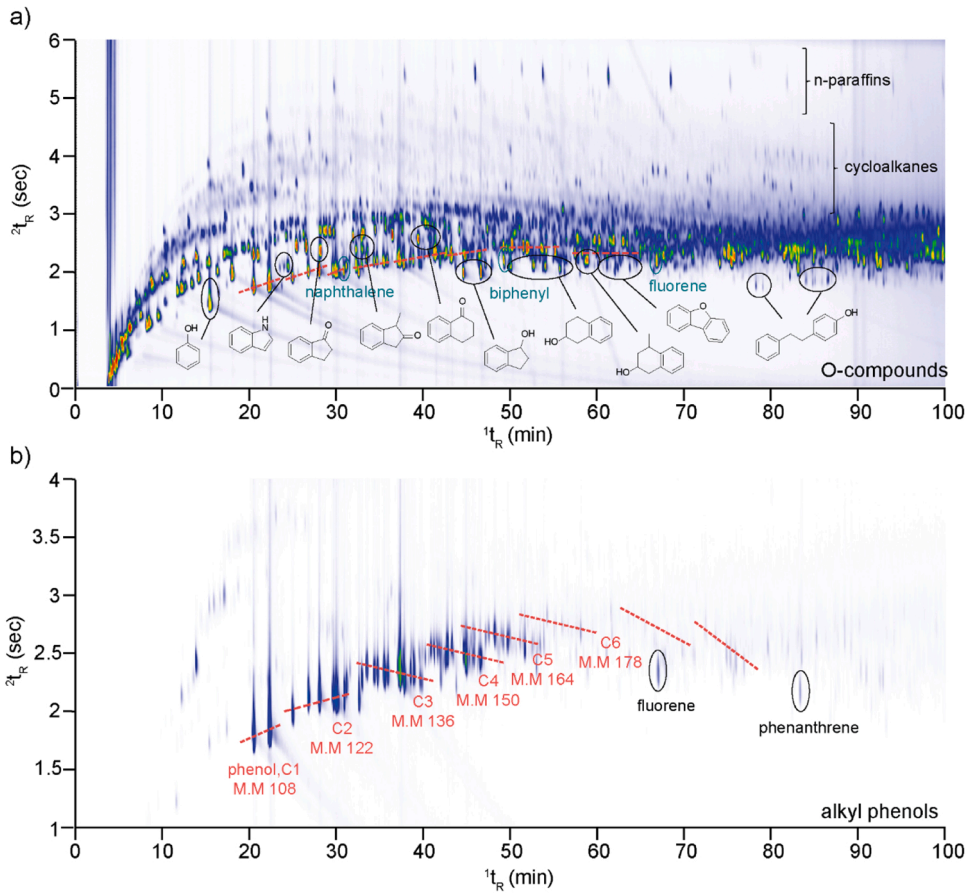

Fig. 4. GC×GC-EI-TOF MS (reverse column set-up) total ion chromatogram (TIC) of (a) HDT-RCFP #6. (b) Extracted ion chromatograms illustrating the detection of alkyl phenols for the HDT-RCFP #6 sample.

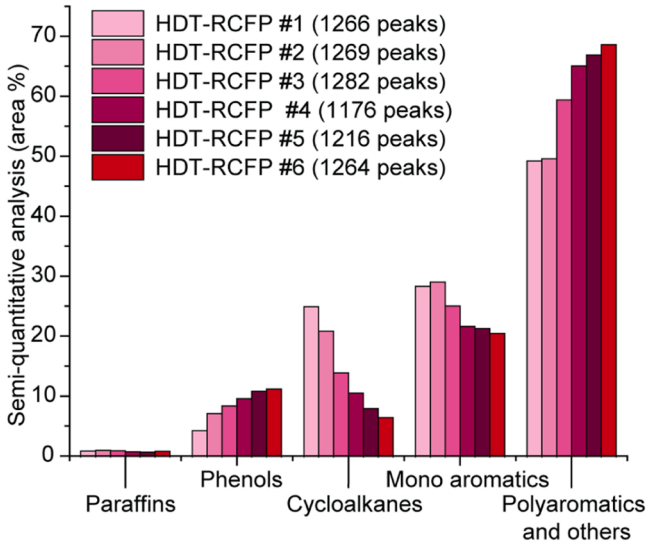

Fig. 5. Comparison of the chemical class distribution (percent area) among the six HDT-effluents obtained by GC×GC-EI-QTOF MS in normal phase set-up. The number of peaks detected in each effluent is also described. Samples HDT-RCFP #1 to #6 represent the effluents collected at the different time points, respectively at 48.5, 72.5, 96.5, 124.5, and 143.5 hours.

4. Conclusions

This study demonstrated the complementary chemical analyses that can be performed using reverse and normal phase column configurations in GC×GC MS for the characterization of volatile compounds in upgraded pyrolysis bio-oils. Identifying and semi-quantifying hydrocarbon and oxygen compounds using these configurations contributed to a better understanding of the catalyst deactivation during the hydrotreatment process of bio-oils. A clear step change in chemical composition was observed at a specific time during the hydrotreatment process. The relative concentration of polyaromatic hydrocarbons increased significantly, while the relative concentration of cycloalkanes and monoaromatics decreased. Additionally, the amount and diversity of oxygenated components also increased significantly over time. From an industrial point of view, these observations provide additional insights for adapting catalysts and processing conditions to improve the bio-oil hydrotreatment process.

CRediT authorship contribution statement

Eliane Lazzari: Writing – review & editing, Writing – original draft, Visualization, Validation, Resources, Methodology, Investigation, Data curation, Conceptualization. **Jean-François Focant:** Writing – review & editing, Methodology. **Giorgia Purcaro:** Writing – review & editing, Methodology, Conceptualization. **Pierre Giusti:** Writing – review & editing, Validation, Supervision, Project administration, Investigation, Funding acquisition, Conceptualization. **Marco Piparo:** Writing – review & editing, Validation, Supervision, Project administration, Methodology, Funding acquisition, Conceptualization. **David C. Dayton:** Writing – review & editing, Supervision, Project administration,

Funding acquisition, Conceptualization. **Charlotte Mase:** Writing – review & editing, Writing – original draft, Visualization, Validation, Resources, Methodology, Investigation. **Sabrina Marceau:** Validation, Resources, Methodology, Investigation, Data curation.

Declaration of Competing Interest

The authors declare that they have no known competing financial interests or personal relationships that could have appeared to influence the work reported in this paper.

Data Availability

Data will be made available on request.

Acknowledgements

The authors thank JEOL Ltd., and GL Sciences for the support on instrumentation. The authors thank RTI International for providing the samples.

Appendix A. Supporting information

Supplementary data associated with this article can be found in the online version at doi:10.1016/j.jaap.2024.106569.

References

[1] V. Dhyani, T. Bhaskar, Renew. Energy 129 (2018) 695, https://doi.org/10.1016/j.renene.2017.04.035.
[2] A.V. Bridgwater, D. Meier, D. Radlein, Org. Geochem. 30 (1999) 1479, https://doi.org/10.1016/s0146-6380(99)00120-5.
[3] C. Liu, H. Wang, A.M. Karim, J. Sun, Y. Wang, Chem. Soc. Rev. 43 (2014) 7594, https://doi.org/10.1039/c3cs60414d.
[4] K. Wang, D.C. Dayton, J.E. Peters, O.D. Mante, Green. Chem. 19 (2017) 3243, https://doi.org/10.1039/c7gc01088e.
[5] D.C. Dayton, O.D. Mante, J. Weiner, C. Komnaris, S. Verdier, J. Gabrielsen, Energy Fuels 36 (2022) 9147, https://doi.org/10.1021/acs.energyfuels.2c01753.
[6] P. Cross, K. Wang, J. Weiner, E. Reid, J. Peters, O. Mante, D.C. Dayton, Energy Fuels 34 (2020) 4678, https://doi.org/10.1021/acs.energyfuels.0c00320.
[7] A.V. Bridgwater, Biomass Bioenergy 38 (2012) 68, https://doi.org/10.1016/j.biombioe.2011.01.048.
[8] Y. Yang, X. Xu, H. He, D. Huo, X. Li, L. Dai, C. Si, Int. J. Biol. Macromol. 242 (2023) 124773, https://doi.org/10.1016/j.ijbiomac.2023.124773.
[9] H. Lee, Y.-M. Kim, I.-G. Lee, J.-K. Jeon, S.-C. Jung, J.D. Chung, W.G. Choi, Y.-K. Park, Korean J. Chem. Eng. 33 (2016) 3299, https://doi.org/10.1007/s11814-016-0214-3.
[10] Y. Wang, Y. Han, W. Hu, D. Fu, G. Wang, J. Sep Sci. 43 (2020) 360, https://doi.org/10.1002/jssc.201901014.
[11] C.M. Michailof, K.G. Kalogiannis, T. Sfetsas, D.T. Patiaka, A.A. Lappas, WIREs Energy Environ. 5 (2016) 614, https://doi.org/10.1002/wene.208.
[12] J. Hertzog, C. Mase, M. Hubert-Roux, C. Afonso, P. Giusti, C. Barrère-Mangote, Energy Fuels 35 (2021) 17979, https://doi.org/10.1021/acs.energyfuels.1c02098.
[13] M. Staš, M. Auersvald, L. Kejla, D. Vrtiška, J. Kroufek, D. Kubička, TrAC Trends Anal. Chem. 126 (2020), https://doi.org/10.1016/j.trac.2020.115857.
[14] M. Staš, J. Chudoba, D. Kubička, J. Blažek, M. Pospíšil, Energy Fuels 31 (2017) 10283, https://doi.org/10.1021/acs.energyfuels.7b00826.
[15] P.K. Kanaujia, Y. Sharma, M. Garg, D. Tripathi, R. Singh, J. Anal. Appl. Pyrol. 105 (2014) 55.
[16] P.K. Kanaujia, Y.K. Sharma, U.C. Agrawal, M.O. Garg, TrAC Trends Anal. Chem. 42 (2013) 125, https://doi.org/10.1016/j.trac.2012.09.009.
[17] N.S. Tessarolo, L.R. dos Santos, R.S. Silva, D.A. Azevedo, J. Chromatogr. A 1279 (2013) 68, https://doi.org/10.1016/j.chroma.2012.12.052.
[18] M. Staš, M. Auersvald, P. Vozka, Energy Fuels 35 (2021) 8541, https://doi.org/10.1021/acs.energyfuels.1c00553.
[19] T.K. Dada, M. Sheehan, S. Murugavelh, E. Antunes, Biomass Convers. Bioref. 13 (2023) 2595, https://doi.org/10.1007/s13399-021-01391-3.
[20] M.R. Djokic, T. Dijkmans, G. Yildiz, W. Prins, K.M. Van Geem, J. Chromatogr. A 1257 (2012) 131, https://doi.org/10.1016/j.chroma.2012.07.035.
[21] M. Beccaria, A.L.M. Siqueira, A. Maniquet, P. Giusti, M. Piparo, P.H. Stefanuto, J. F. Focant, J. Sep Sci. 44 (2021) 115, https://doi.org/10.1002/jssc.202000907.
[22] M. Beccaria, Y. Zou, P.-H. Stefanuto, A.L.M. Siqueira, A. Maniquet, M. Piparo, P. Giusti, G. Purcaro, J.-F. Focant, Talanta 238 (2022), https://doi.org/10.1016/j.talanta.2021.123019.
[23] B. Omais, J. Crepier, N. Charon, M. Courtiade, A. Quignard, D. Thiebaut, Analyst 138 (2013) 2258, https://doi.org/10.1039/c2an35597c.
[24] A. Giri, M. Coutriade, A. Racaud, P.H. Stefanuto, K. Okuda, J. Dane, R.B. Cody, J. F. Focant, J. Mass Spectrom. 54 (2019) 148, https://doi.org/10.1002/jms.4319.
[25] M. Beccaria, M. Piparo, Y. Zou, P.H. Stefanuto, G. Purcaro, A.L. Mendes Siqueira, A. Maniquet, P. Giusti, J.F. Focant, Talanta 252 (2023) 123799, https://doi.org/10.1016/j.talanta.2022.123799.
[26] E. Lazzari, M. Piparo, C. Mase, L. Levacher, P.-H. Stefanuto, G. Purcaro, J.-F. Focant, P. Giusti, J. Anal. Appl. Pyrolysis 176 (2023), https://doi.org/10.1016/j.jaap.2023.106224.
[27] M.L. Chacón-Patiño, C. Mase, J.F. Maillard, C. Barrère-Mangote, D.C. Dayton, C. Afonso, P. Giusti, R.P. Rodgers, Energy Fuels 37 (2023) 16612, https://doi.org/10.1021/acs.energyfuels.3c02599.
[28] A. Giri, M. Coutriade, A. Racaud, K. Okuda, J. Dane, R.B. Cody, J.F. Focant, Anal. Chem. 89 (2017) 5395, https://doi.org/10.1021/acs.analchem.7b00124.
[29] A. Shimoyama, H. Yabuta, Geochem. J. 36 (2002) 173, https://doi.org/10.2343/geochemj.36.173.
[30] H. Yabuta, H. Mita, A. Shimoyama, Geochem. J. 36 (2002) 31, https://doi.org/10.2343/geochemj.36.31.
[31] M.S. Alam, C. Stark, R.M. Harrison, Anal. Chem. 88 (2016) 4211, https://doi.org/10.1021/acs.analchem.5b03122.
[32] Z. Yang, Z. Xu, M. Feng, J.R. Cort, R. Gieleciak, J. Heyne, B. Yang, Fuel 321 (2022), https://doi.org/10.1016/j.fuel.2022.124040.
[33] B. Omais, M. Courtiade, N. Charon, D. Thiebaut, A. Quignard, M.C. Hennion, J. Chromatogr. A 1218 (2011) 3233, https://doi.org/10.1016/j.chroma.2010.12.049.
[34] B. Joffres, M.T. Nguyen, D. Laurenti, C. Lorentz, V. Souchon, N. Charon, A. Daudin, A. Quignard, C. Geantet, Appl. Catal. B: Environ. 184 (2016) 153, https://doi.org/10.1016/j.apcatb.2015.11.005.
[35] P.Q. Tranchida, A. Casilli, P. Dugo, G. Dugo, L. Mondello, Anal. Chem. 79 (2007) 2266, https://doi.org/10.1021/ac0618066.
[36] A. Mostafa, M. Edwards, T. Gorecki, J. Chromatogr. A 1255 (2012) 38, https://doi.org/10.1016/j.chroma.2012.02.064.
[37] A. Korban, R. Čabala, V. Egorov, Z. Bosáková, S. Charapitsa, Talanta 246 (2022) 123518, https://doi.org/10.1016/j.talanta.2022.123518.